

Energetics and Dynamics of a stable Bloch point

Thomas Brian Winkler^{1*}, Marijan Beg², Martin Lang^{3,4}, Mathias Kläui^{1*}, Hans Fangohr^{3,4*}

1 - Institute of Physics, Johannes Gutenberg University, Staudinger Weg 7, 55128 Mainz, Germany

2 - Department of Earth Science and Engineering, Imperial College London, London SW7 2AZ, United Kingdom

3 - Faculty of Engineering and Physical Sciences, University of Southampton, University Road, Southampton SO17 1BK, United Kingdom

4 - Max Planck Institute for the Structure and Dynamics of Matter Hamburg, Luruper Chaussee 149, 22761 Hamburg, Germany

* Email: twinkler@uni-mainz.de, klaeui@uni-mainz.de, hans.fangohr@mpsd.mpg.de

Abstract

Magnetic Bloch points (BPs) are highly confined magnetization configurations, that often occur in transient spin dynamics processes. However, opposing chiralities of adjacent layers for instance in a FeGe bilayer stack can stabilize such magnetic BPs at the layer interface. These BPs configurations are metastable and consist of two coupled vortices (one in each layer) with same circularity and opposite polarity. Each vortex is stabilized by opposite sign Dzyaloshinskii-Moriya interactions. This stabilization mechanism potentially opens the door towards BP-based spintronic applications. An open question, from a methodological point of view, is whether the Heisenberg (HB) model approach (atomistic model) as to be used to study such systems or if the -- computationally more efficient -- micromagnetic (MM) models can be used and still obtain robust results. We are modelling and comparing the energetics and dynamics of a stable BP obtained using both HB and MM approaches. We find that an MM description of a stable BP leads qualitatively to the same results as the HB description, and that an appropriate mesh discretization plays a more important role than the chosen model. Further, we study the dynamics by shifting the BP with an applied in-plane field and

investigating the relaxation after switching the field off abruptly. The precessional motion of coupled vortices in a BP state can be drastically reduced compared to a classical vortex, which may be also an interesting feature for fast and efficient devices. A recent study has shown that a bilayer stack hosting BPs can be used to retain information [1].

Introduction

Studying magnetic thin-film and multilayer-stack systems on the mesoscopic scale is of fundamental interest for researchers in basic science as well as for applications. On the one hand, the investigation of topologically protected spin structures, such as Skyrmions [2] or Hopfions [3], and their manipulation with fields and spin-currents allows for analysing the dynamics of topological quasi-particles as well as spin phenomena. On the other hand, the realization of low-power and high-density next-generation storage devices and implementation of neuromorphic computing schemes into such systems is of huge economic relevance and also for ecological reasons of interest [4–6].

The Dzyaloshinskii-Moriya interaction (DMI) plays a key role for the stabilization of magnetic solitons [7]. This indirect, asymmetric exchange interaction favors spin canting between neighboring spins and gives rise to a certain chirality and topologically stabilized spin structures [2].

In our investigation, we focus on the most highly confined soliton, a Bloch point (BP) [1,8–10]. A BP is a magnetic singularity, a point where the magnetization \mathbf{m} diverges. BPs commonly occur in transient spin dynamics processes [11] but are usually not stable as static spin structures in thin films. However, in a simulation-based study Beg et al. [8] were able to show that a BP can be stabilized in a by stacking on top of each other two FeGe layers with opposite sign of the (bulk) DM energy constant D . A magnetic vortex forms in each layer. The two vortices – one in each layer – have identical circularity and opposite polarity to satisfy the respective material constant D (and the associated chirality) of their hosting layer. A vortex typically has four energetically equal states, defined by a combination of the circularity c (± 1) and polarity p (± 1). In a material with DMI, two combinations of c and p are energetically more favorable (the chirality of DMI couples circularity

and polarization). Stacking two layers with DMI strengths D_1 and $D_2 = -D_1$, the DMI energy can stabilize two vortices with same circularity but different polarity, leading to a BP at the interface between the top (D_1) and bottom (D_2). So, the preferred handedness in each layer is established at the cost of one magnetic singularity. In our case, we find a Head-to-Head BP (HH-BP) an illustration is shown in **Fig. 1a**.

It is unclear if a BP can be investigated within a micromagnetic model (MM) approach, due to the strong spatial variations of the magnetization field [11,12]. MM results may be not robust when the spin canting between neighboring simulations cells increases above a certain angle, for both finite-element and finite-difference approaches. Atomistic or multi-scale simulations [11–14] are better suited to investigate such systems. However, theoretical and numerical investigations have been previously carried out to analyse a BP also within the MM framework [8,15–17]. In Ref. [15], the authors showed that the existence of a Bloch point during a vortex core reversal in an MM framework is possible. However, the calculated energy barriers are dependent on the mesh discretization, indicating potential issues with this approach. In [16], the authors were able to predict the existence of chiral bobbars in an MM framework, a stable spin structure containing a BP. In a recent publications A. Savchenko *et al.* showed the existence of a “Dipole string” in an FeGe cylinder [18], a magnetization configuration containing two BPs, experimentally observed by transmission electron microscopy. To model fabrication defects, the DMI was switched off at the surface of the cylinder. This is related to our approach of inducing BPs by modelling different regions with different DMI strengths.

A more accurate model than the MM model to describe such a system with spatially strongly varying magnetization is the Heisenberg (HB) model, which allows one to simulate every magnetic unit cell with its interactions. The HB model inherently can deal with arbitrary variations of the spin structure. The MM model is derived from the HB model and assumes a spatially slowly varying magnetization. The drawback of the HB model is the high computational effort, since every magnetic unit cell is simulated separately, while in a MM framework a system discretization can be chosen that requires

up to several orders of magnitude fewer simulation cells than the HB model (depending on the magnetic parameters).

In this work, we systematically study the energetics and dynamics of a stable BP in a bilayer stack within the MM framework and compare the results with the more accurate HB model. A key parameter for us is the mesh discretization d , which is varied from a few nm down to a few Å. We on purpose also choose discretizations d smaller than the atomic lattice constant $a = 0.4679$ nm for FeGe, to probe the MM framework. For a detailed discussion on the fundamental differences between the MM and the HB model in our implementation, we refer to Ref. [11].

The study consists two parts: First, we nucleate a stable Bloch point according to [8] and calculate the energy obtained for different discretizations. As a comparison we also nucleate a vortex in the bilayer system. This “bilayer vortex” – a vortex extending over both layers with same polarity and circularity in both layers – enables us to compare the BP configuration’s behaviour with that of a configuration

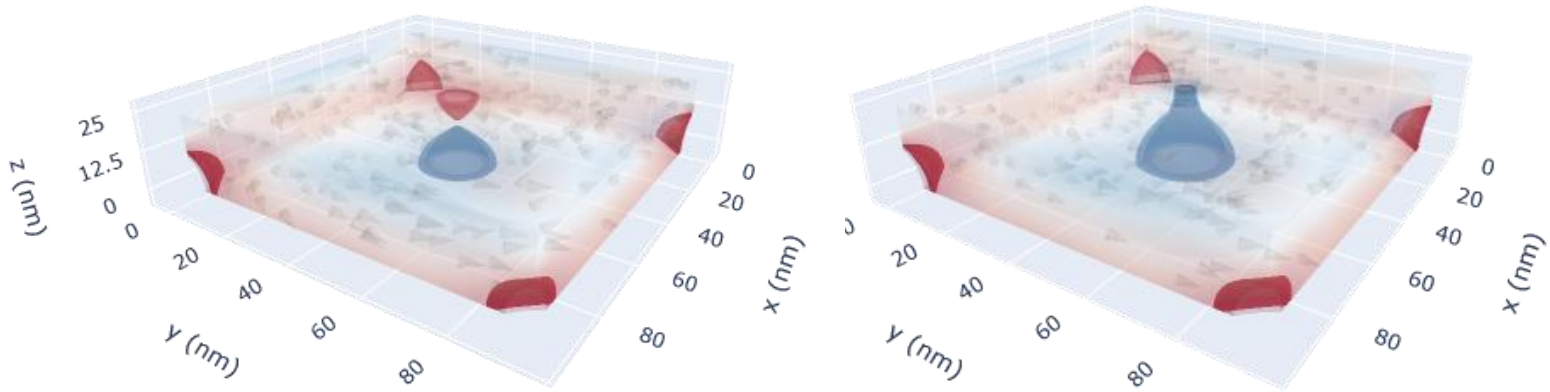


Figure 1: Two of the investigated structures in a square-shaped geometry. BP state (left) and

bilayer vortex state (right) are both stable in the bilayer stack. The isosurfaces show magnetization with $m_z < -0.85$ (red) or $m_z > 0.85$ (blue). Grey cones visualize the in-plane magnetization. Not every simulation cell is plotted. Due to the rectangular shape and the DMI, the bottom corners also show a large OOP component.

that is generally accepted to be accurately described within the MM model. We use a third system for further comparisons: here, we nucleate a vortex in the same geometry and material but have artificially set the DM constant to zero (in both layers). This third system is comparable to a

Permalloy material and connects this work to all the “classic” vortex studies from past decades (often carried out on materials such as Permalloy). To minimize shape approximation errors in the finite-difference method, we use a square-shaped nano-scale geometry.

In the second part, we move the stable BP with an external field applied in-plane (IP) with a strength of 25mT. We then switch off the field and analyze the relaxation process of the BP. We compare the dynamics with a classic magnetic vortex in FeGe, without DMI, and the vortex in the bilayer-stack. Again, we vary the mesh discretization to probe the MM framework. For this part of the study, a circular-shaped nano-disk is chosen to make results of the vortex motion more comparable with analytical solutions or calculations based on the Thiele model [19].

Methods

Our simulation-based study is mainly done with MicroMagnum [20,21], a free, open source simulation package, that allows for fast GPU-accelerated time integration with double-precision. The fast calculation of the stray field is done with the FFTW package [22]. However, many in-house extensions have been made in the recent years [11,14,23] to adapt the code to today’s research interests, such as the DMI interaction. In particular, the HB model was included to allow for accurate simulation of spin structures that are normally outside the scope of the MM framework.

MicroMagnum uses the finite-difference method and the Runge-Kutta evolver of fifth order for the time integration.

The study is considering an FeGe bilayer-stack and we adopt all material parameters from [8]. The evaluated energy contributions are the exchange energy ($A = 8.78$ pJ/m), the demagnetization field ($M_s = 0.384$ MA/m) and the DMI ($D_1 = -D_2 = 1.58$ mJ/m²) with opposite sign in each of the layers. The thicker bottom layer ($D_1 > 0$) has a thickness of $t_{\text{bottom}} = 30 \cdot a$, the thinner top layer ($D_1 < 0$) a thickness of $t_{\text{bottom}} = 20 \cdot a$, resulting in a 3/2 ratio, enabling us to vary the MM

discretization in reasonably many steps without distracting the ratio of the layers in the MM framework. The side-length l of the square-shaped geometry was chosen as $l = 200 \cdot a$.

To move the BP, the bilayer vortex and the vortex in the respective simulated samples out of equilibrium, we use an external magnetic field.

To nucleate the BP, we initialize the system as homogeneously magnetized in the z direction. Then we let the system evolve according to the Landau-Lifshitz-Gilbert-equation [24,25]. To nucleate the vortex in the bilayer stack, we also initialize the system in the z direction and then relax with the dissipative LLG equation (without the precessional term). For nucleating the classical magnetic vortex, we initialize the system with an analytical expression that approximates a vortex configuration and then let the system evolve. All relaxations are performed with a stopping criterion of a maximum torque of $\tau = 0.5$ degree/ns. The important length scales for choosing the discretization are the exchange length $l_{\text{ex}} = \sqrt{(2A/\mu_0 M_s^2)} = 9.73$ nm, the helical length $L_D = \frac{4\pi A}{D} = 70$ nm and the atomic lattice constant of FeGe, $a = 0.4679$ nm. We choose MM discretizations below l_{ex} and even below a to probe the stability of the BP in the MM framework.

Results and Discussion

Energy of the BP state

Beg et al. have shown that a stable BP can be nucleated in an MM framework [8]. We repeat the simulation for different cell sizes in the MM framework, as well as in the HB model. We compare the energy of the stable BP with a bilayer vortex in the same system. The latter configuration would widely be regarded as a structure that can be modelled using micromagnetics, and we use it as a comparison system to provide context for the observed inaccuracies. **Fig. 2a** shows the total energy, and the single energy terms for our studied system and the comparator systems on the y -axis. On the x -axes, we vary the MM discretisation between $d_{\text{max}} = 10 \cdot a = 4.679$ nm and $d_{\text{min}} \approx 0.2599$ nm.

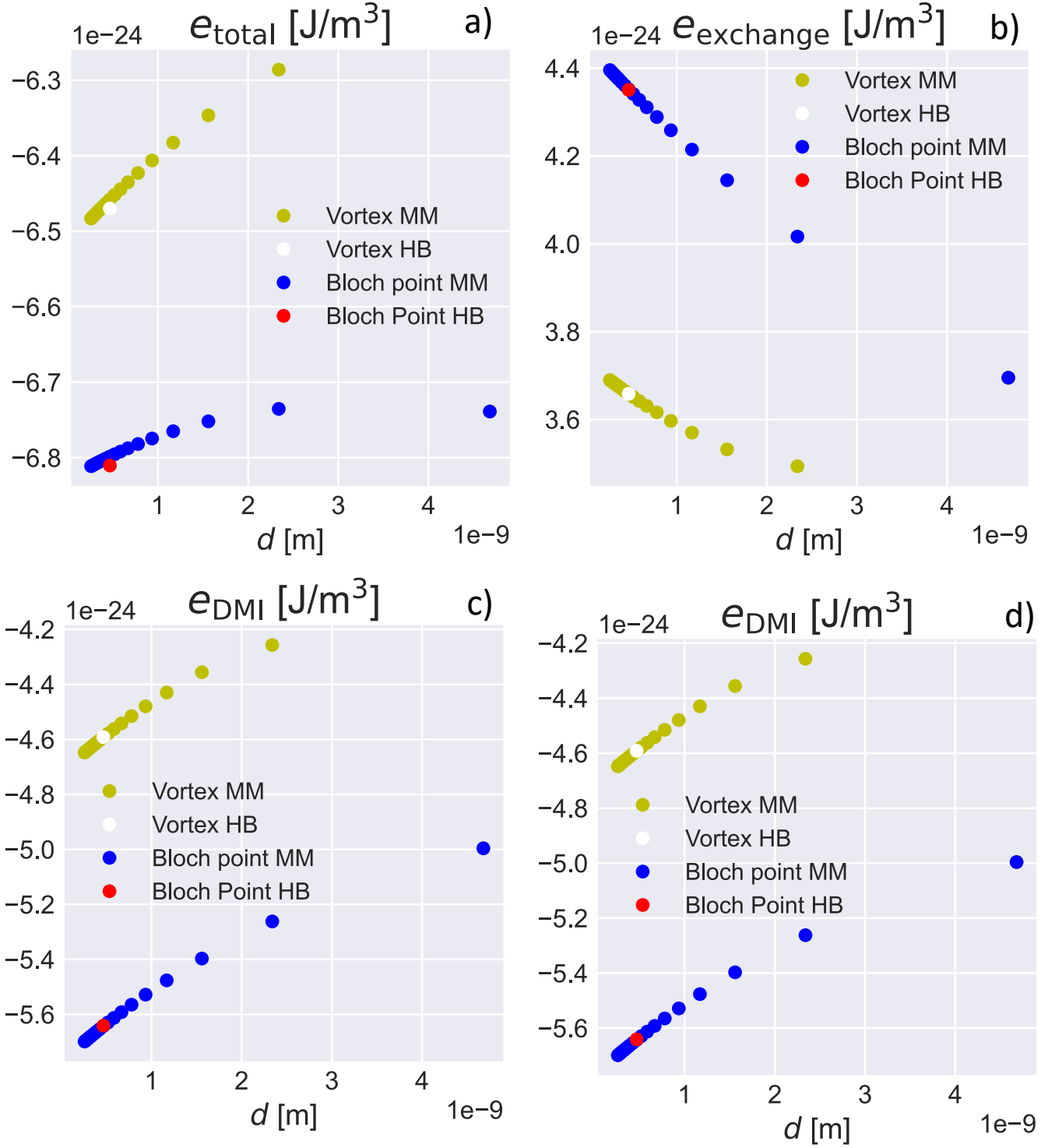


Figure 2 a) - d): total energy density and single contributions for the BP state and the bilayer vortex state, for various discretizations in the MM model and the more accurate HB model. It is clearly visible that the MM energy approaches the HB value for decreasing simulation cell size.

We note that the BP configuration has a lower energy than the bilayer-vortex configuration. Both, **Fig. 2** configurations are stable for all chosen discretizations. From **Fig. 2d**, we see that the DMI energy in the BP state is minimized compared to the vortex state. As the material has two DMI constants of opposite sign, the bilayer vortex state has the less favoured handedness in one of the layers, whereas the Bloch point configuration minimises exactly that energy through aligning the handedness of the vortices in bottom and top layer with the preferred handedness of the DMI material constants. **Fig. 2b** shows that the exchange energy of the BP configuration is higher than that of the bilayer vortex configuration. The Bloch point itself contributes to this increased exchange energy density. In absolute numbers, the difference in energy density due to the exchange is about an order of magnitude smaller than the difference in the DMI term. The presence of the Bloch point also increases the stray field energy density a little (**Fig. 2c**). Overall, the energy reduction in the DMI energy density for the BP configuration outweighs the increments of energy for the stray field and the exchange energy. This is in line with Ref. [8] who reports the BP as the stable configuration with the lowest energy.

We note that for the largest chosen MM cell size of $d_{MM} = 10 \cdot a = 4.679 \text{ nm}$ the bilayer vortex state is not stable, but only the BP state exists in equilibrium.

The total energy is decreasing in both systems with decreasing cell size (**Fig. 2a**). This is reasonable since the circular magnetization in the vortices can align better in a finer grid. The stray field energy is saturating faster for smaller fields (**Fig. 2c**). Due to its long-range nature, it is less sensitive to the mesh discretization.

The trend for the single MM energies for the exchange and the DMI continues if the cell size is chosen to be smaller than the lattice constant a . This is not surprising, since a is an arbitrarily chosen constant from a MM perspective.

To compare energies in the MM and HB model, we have subtracted the energies of the ferromagnetic state from all energy terms. The HB energies are generally in agreement with the MM model, and no qualitative differences are visible. Energy differences between micromagnetic and

Heisenberg model with the same lattice spacing are of the order of 10^{-19} J/m³, suggesting that the discretization is a more important factor for the outcome than the choice of the model. For the important topic of skyrmion stability and skyrmion annihilation processes in circular disks and some related studies also the effects of the discretization have been found to be important highlighting the interest in understanding the validity of such simulations [11,26–28].

Energy of the BP core

The stable BP, a singularity in the MM framework, normally requires the HB model, which can handle diverging spin canting more realistically. To probe the MM framework, we vary the MM cell size of the BP state and explore the energy of the BP. **Fig. 3a** shows the exchange and DMI energy of the 4^3 cells containing the singularity (i.e. 4 cells in each dimension, spanning 64 simulation cells) as a function of the cells size d . The energy is proportional to the volume V of the region, $E \propto V \propto d^3$, where d is the edge length of a discretisation cell. According to Döring [29], the exchange energy density $e_{\text{exch,BP}}$ of a singularity is proportional to $1/d^2$ in a discretised mesh, i.e. $e_{\text{exch,BP}} \propto 1/d^2$, which arises from the squared spatial derivatives in the MM formulation of the exchange energy density, $e_{\text{exch,BP}} = A \cdot (\delta \mathbf{m} / \delta x)^2$. Therefore, we observe a linear dependence of the absolute exchange energy, $E_{\text{exch,BP}} = V \cdot e_{\text{exch,BP}} \propto d^3 \cdot 1/d^2 \propto d$ (see the red line in **Fig. 3a**). Similar considerations can be done for the DMI energy around the center. The MM formulation of the DMI energy density includes only the first spatial derivatives of \mathbf{m} with respect to d , $e_{\text{DMI,BP}} = D \mathbf{m} \cdot (\nabla \times \mathbf{m})$. In contrast to the exchange energy, spin canting minimizes the DMI energy density. Thus, in line with Döring's considerations for the exchange energy, $e_{\text{DMI,BP}} \propto -1/d$. Therefore, we observe a negative quadratic dependence, $E_{\text{DMI,BP}} = V \cdot e_{\text{DMI,BP}} \propto -d^2$, as shown in **Fig. 3a**. This discussion holds, if we can assume that the investigated magnetization structure in the 4^3 discretisation cells does not substantially change for different discretizations d . **Fig. 3b**. shows the maximum angle β of the magnetisation vectors between neighboring discretization cells in the sample as a function of the

inverse cell size, and we see that the angle β observed in the magnetization structures does not substantially vary, indicating a sufficiently similar magnetization structure for similar values of d .

	BP state	BV state
Fit parameter β_{lim}	$72.875 \pm 0.240^\circ$	$1.196 \pm 0.125^\circ$
Fit parameter c	$14.250 \pm 0.354^\circ$	$15.572 \pm 0.301^\circ$

Table 1: Fitting parameter for the curves in Fig. 2b) to find the maximum angle β in a continuous MM model. Fit parameter c is listed for the sake of completeness.

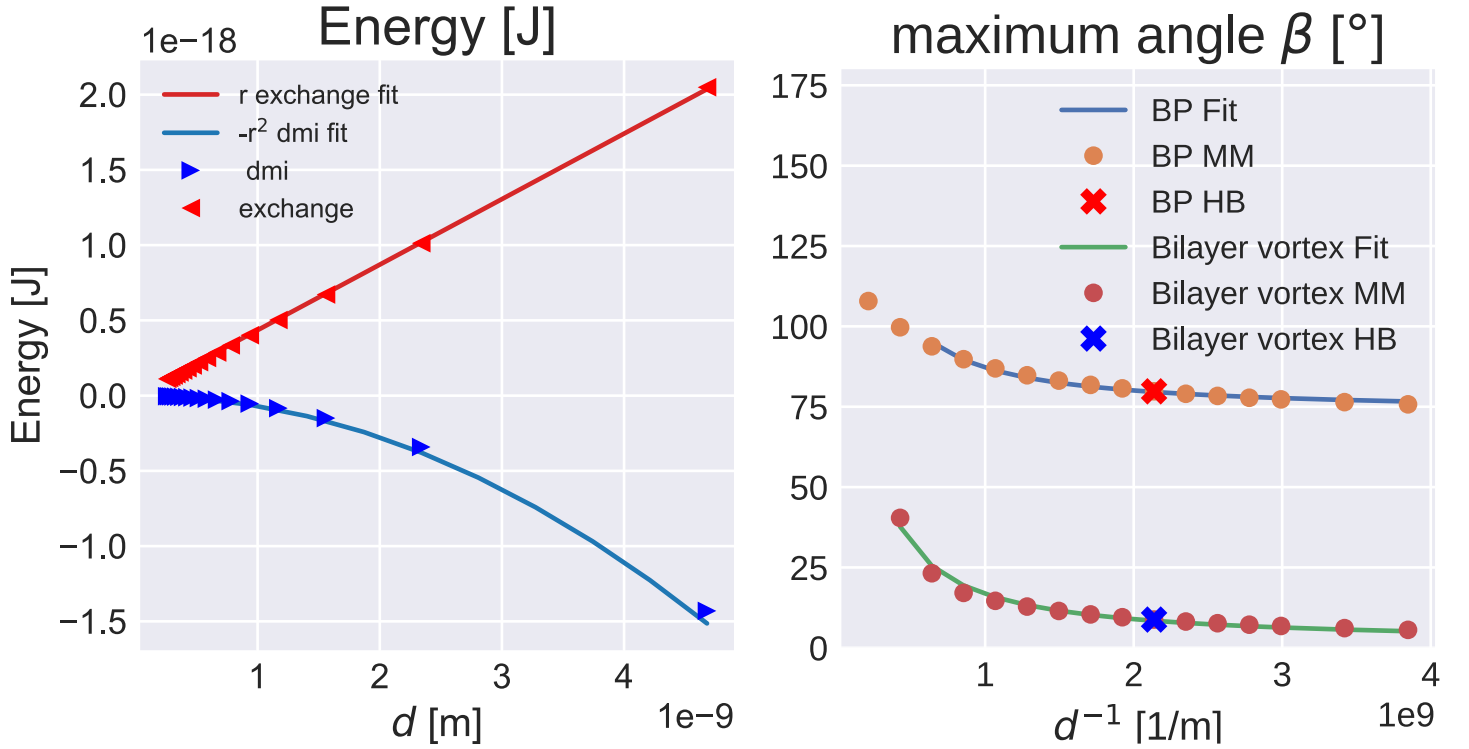


Figure 3: a) The energy contributions of the 4^3 cells around the Bloch point for varying MM cell sizes. According to Döring [29] and the decreasing volume, the absolute exchange energy is decreasing linearly. The DMI energy varies with $-d^2$. In summary, that means that the overall energy contribution of the BP to the BP state gets also negligible. **b)** The maximum angle between all neighboring magnetization vectors (data points with a cross are magnetic moments in the Heisenberg model, HB. All other data points are for magnetization vectors defined in the cells of the finite difference discretization of the micromagnetic model

for different edge lengths d of the discretisation of the cells. The finer the grid, the smaller is the maximum angle of the MM cells that host the BP. The HB simulation results coincide with the MM simulation results for a cell size corresponding to the magnetic moment spacing in the HB model. For smooth magnetization fields we expect a limit $\beta_{lim} \rightarrow 0^\circ$ for $d \rightarrow 0$.

Fig. 3b shows that the maximum angle β is larger for larger cell sizes. This is reasonable since a coarse mesh needs larger changes from cell to cell to achieve the same overall change in the magnetization. We use the following model to fit the data points for the maximum angle $\beta(d^{-1})$ as a function of d^{-1} in **Fig. 3b**: $\beta(d^{-1}) = c \cdot d^{-1} + \beta_{lim}$. We find that for the bilayer vortex, the offset angle $\beta_{lim,BV} = 1.2^\circ$ for the BV system is close to zero for large d^{-1} (i.e. for a small discretisation cell size), see **Tab. 1**. For the Bloch Point (BP) state, we find a corresponding large angle $\beta_{lim,BP} = 72.87^\circ$. The value arises from the discontinuity at the interface, where the BP is located. Theoretical predictions [10,29] are leading to similar values (67.6° and 75.1°), and simulations [13] further confirmed the results (72.3° and 72.3° , dependent on the lattice orientation). The agreement is also a good indication for the reliability of our simulation model.

Dynamics of the stable BP

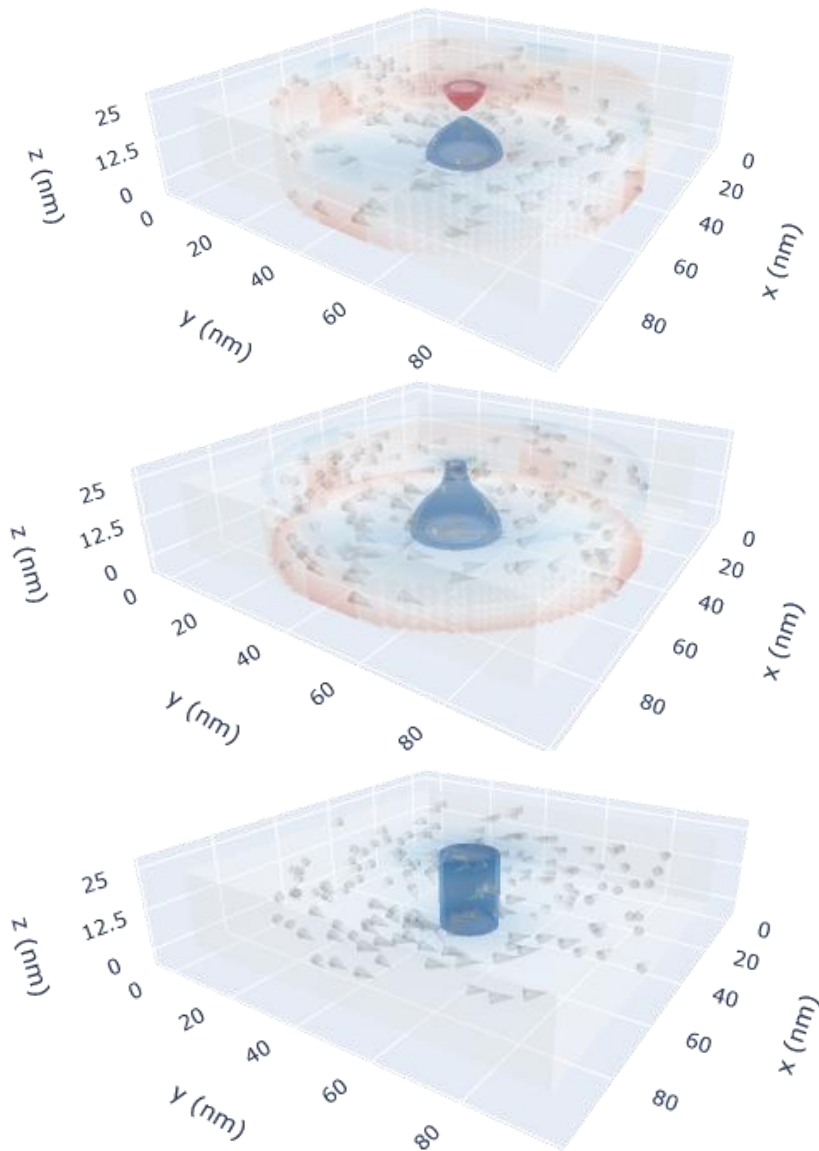
We investigate the dynamics of a stable BP configuration. We start our study from an equilibrium configuration where the BP is located at the interface between the two layers and in the middle of a disk geometry. The initial equilibrium configuration is shown in Figure 4 (left). We then create a higher energy configuration by applying an external field of $H_{ext,x} = 25$ mT which is applied in the x direction. This applied field moves the BP from the initial equilibrium position at the center of the disk to a new location in the x-y plane. When this higher energy configuration has been obtained numerically, we set the external field to zero. At this point, we have changed the energy surface and the magnetization configuration wants to change back into the initial equilibrium configuration. We simulate the time dependence of this process and thus investigate the dynamics of the BP moving

back to the center position (which is the energy minimum). We make a snapshot of the configuration every 20 ps. We further investigate how the discretization in the MM model is influencing the BP movement.

To put the observed BP dynamics into context, we repeat the process of field-shifting, as described above for the BP configuration, with the vortex configuration in the bilayer system, and with a classical vortex (CV) in a FeGe disk (i.e. without any DMI interactions for the classical vortex), where the motion is well-known and can be described analytically. **Fig. 4** visualizes the systems in the equilibrium state without applied field. For the classical vortex we used a field strength of 10 mT to reach a similar displacement of the core compared to the systems containing DMI, which results in a large restoring force. We use circular disks for this part of the study to minimize affecting the

precessional motion by a non-rotational symmetry of the sample shape. The diameter d_{disk} of the disks is chosen with $d_{\text{disk}} = 200 \cdot a$.

Figure 4: The three investigated structures in a cylindrical disk. The BP state in the bilayer system (left), the vortex state in the bilayer system (middle) and a classical vortex in a one-layer stack without DMI, where motion can be described analytically.



The position of the vortex in one z-slice of a simulation is calculated by the center of mass of the topological charge density, calculated with the Berg-Lüscher method [30]. In more detail, an initial guess of the vortex position is given through the weighted mean of the 4 cells with the highest absolute z-magnetization, with the z-magnetization chosen as weights. A cut-off radius around this first approximation of the vortex position is chosen with $r_{\text{cutoff}} = 1/4 r_{\text{disk}}$. Within this region the topological charge density is calculated. The cut-off is used to not disguise the center position by the significant edge canting that occurs in these finite-size DMI systems. For the vortex configurations, the position is calculated on a x-y data set that is obtained by averaging all vectors at that x-y position in the z-direction.

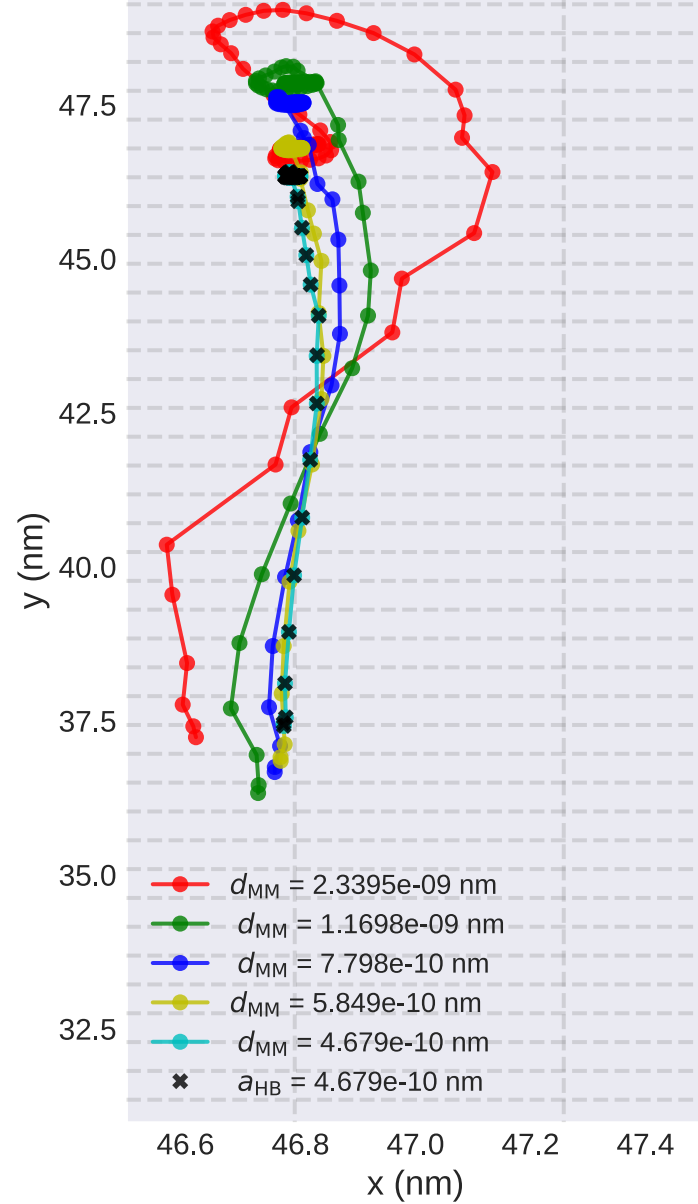
To compute the BP position, we re-use the algorithm described above for the vortex position calculation as the BP consists of one vortex in the top layer and a second vortex in the bottom layer. The BP position is defined as the mean position of these two vortex positions.

Fig. 5 shows the movement of the BP for different discretizations of the MM mesh and within the HB model from its higher energy state back to the center of the geometry as detailed above. The center of the disk is at $y \sim 46.79$ nm. The initial points of the trajectories are found for values of $y < 37.5$ nm due to the field acting in x-direction: By moving the vortex configuration in the y-direction more of the magnetisation can align with the external field. The sign of the displacement along the y-direction is determined by the circularity in the vortex configurations that make up the BP configuration. The figure shows the trajectories once the external field is switched off. We see that for the BP state, the motion shows to first approximation a straight line from the initial to the final point (note the high resolution of the x-scale). The line becomes more straight for smaller micromagnetic discretisation cell sizes. For a discretisation cell size identical to the one used in the Heisenberg model, the Heisenberg model trajectory and the micromagnetic trajectory coincide.

The simulation grid of the Heisenberg model is shown in **Fig. 5** with grey grid lines. We can see that the error that is introduced by using a micromagnetic model with a lattice spacing larger than the

atomistic lattice spacing a_{HB} , that used in the Heisenberg model, is relatively small and of the order of one lattice spacing or smaller in x-direction.

Figure 5: The motion of the BP for different cell sizes and models. Every point indicates a time integration of 20 ps. We see that the BP is moving straight to the center of the disk after turning off the field abruptly. There is no significant precession visible. The dynamics are well described in the MM model when the cell size approaches the HB lattice constant. The underlying grid shows the HB mesh for comparison.



To compare the BP trajectory with that of better-known magnetisation configurations, **Fig. 6a** shows the trajectories of the BP in the bilayer system (which was already discussed in **Fig. 5**), the vortex in the bilayer system and the classical vortex (i.e., without any DMI) within the disk geometry. All results shown

in this figure have been computed using the Heisenberg model, which we treat in this study as the most accurate model available. We use a maximum torque of 0.5 degrees/ns as the stopping criterion for the time integration.

Fig. 6b shows a magnified view of the different trajectories. Also, the motion of the top (green) and bottom (blue) slice of the coupled vortices in the BP state is visualized there. The vortex in the bilayer

system (orange) is exhibiting precession around the center point as would be expected from a vortex configuration [31]. The classical vortex configuration (grey-blue) follows a very similar trajectory.

As visible in **Fig. 6c**, the relaxation of the bilayer vortex (BV) configuration takes more time, $t_{\text{relax}} \approx 3.34$ ns, than the BP configuration ($t_{\text{relax}} \approx 1.66$ ns) and travels a larger distance. A large part of the distance is covered quite rapidly, while the final relaxation close to the equilibrium takes much more time due to the flat energy landscape around the equilibrium position. The classical vortex executes a similar polarity-dependent precession [32] – after removal of an applied field of 10 mT - while relaxing in 4.47 ns. The difference in the relaxation time of the classic vortex and the bilayer vortex might originate from the bilayer vortex's precession being suppressed in the layer in which the chirality of the vortex is opposite to that of the material constant D .

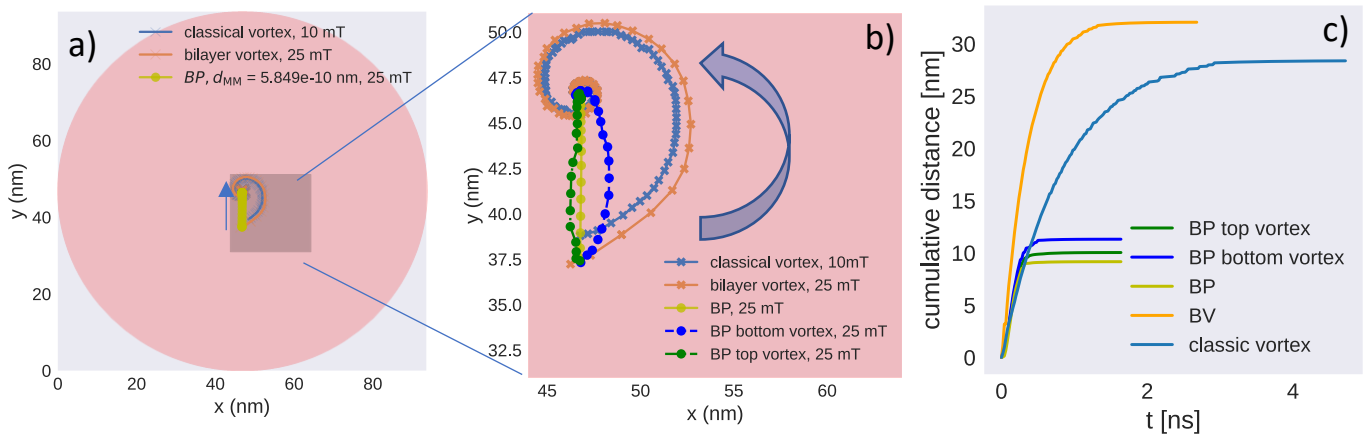


Figure 6: Comparison of the motion of the BP, the bilayer vortex, and the classical vortex in the HB model. Every point indicates a time step of 20 ps . The vortices show typical precession around the center point, while the BP trajectory is leading straight to the center. Blue arrows indicate the direction of motion. **a)** The whole cylindrical disk is shown for a good view on the scales of the movement. **b)** Zoomed into the central region to better see the trajectories. Here, we have added the trajectory of the vortex configuration in the bottom layer (blue) that represents the bottom part of the BP configuration and separately the trajectory of the vortex configuration in the top layer (green) that represents the top part of the BP configuration. We see that they follow a highly damped precession, while the precessional damping is smaller for the larger of the coupled vortices. **c)** The cumulative

travelled distance of the investigated quasi-particles. The vortices in the bilayer system relax much faster into the equilibrium state than the classical vortex and experiences higher velocities.

The motion of the two vortices (one in each layer) that form the BP is shown in green (BP top vortex) and blue (BP bottom vortex) in **Fig. 6b** and **c**. Both vortices show a precession in opposite directions due to their opposite polarity. However, the precession is significantly damped (in comparison to the vortex configurations) due to the coupling of the two vortices that want to precess in opposite directions at the layer interface. The bottom layer shows a larger amount of precession motion; presumably this can be attributed to the bottom layer being thicker than the top layer, and thus giving the vortex configuration more freedom to deviate from the configuration at the layer interface. Next, we check if the precession of two vortices in opposite directions can rupture the Bloch point configuration. We have calculated the largest distance between the vortex core position in the lowest discretisation plane in the top layer (i.e. just above the layer interface) and the vortex core position in highest discretisation plane (i.e. just below the layer interface) and find this to be 0.173 nm in the HB model. So, the vortices can be considered to stay coupled across the layer interface during the relaxation. The deviation observed in **Fig. 6b** originates from a deformation of the vortices further away from the layer interface. The BP trajectory (olive green in **Fig. 6b**) appears as a straight line although the two coupled vortices have different lengths in our system (ratio 3/2, given by the relative thickness of the two stacks). The BP motion is thus for our system not influenced significantly by the two vortex tubes of different lengths.

Conclusion

We have shown, using a Heisenberg model, that the BP configuration has a lower energy than a vortex state in the bilayer system, and is a stable configuration. The vortex state has higher energy, since the DMI energy can only be minimized for one of the two layers. The micromagnetic framework

can yield (at least qualitatively) correct results for the Bloch point system studied here. With finer discretization of the finite-difference mesh the micromagnetic results approach the gold standard results of the HB model quantitatively.

The energies predicted by the micromagnetic model depend weakly on the lattice discretisation used. This is similarly the case for the Bloch point system in a DMI material but also for a vortex configuration in a ferromagnetic material – one of the areas in which micromagnetic simulations are traditionally used as the work horse of computational support for research and development. The energies predicted by the micromagnetic model when using the same lattice spacing as in the Heisenberg model are very close to the energies obtained from the Heisenberg model.

While studying the dynamics of the BP, we find that the motion of the BP is along a straight line whereas a vortex configuration shows precessional motion. The BP is composed of two vortices with identical circularity and opposite polarity. The BP configuration and the exchange coupling of the two vortices across the bilayer interface results in the straight trajectory where the opposite expected motion in the individual layers cancel out. The Bloch point also does not overshoot as known for vortex systems due to their precessional motion. Fast relaxation of solitons may be an important feature for potential applications in storage and computing devices.

Acknowledgment

The group in Mainz acknowledges funding by the emergent AI center, funded by Carl-Zeiss Stiftung, and by and the German Research Foundation (DFG SFB TRR 173 project A01 and B02, 49741853 and 268565370, SPIN+X). This work was financially supported by the EPSRC Programme grant on Skyrmionics (EP/N032128/1).

Authors contributions

Thomas Brian Winkler performed the study and wrote the manuscript. M.B. and H.F. conceived the study. M.K. and H.F. supervised the study. All authors contributed to the project with discussions and contributed to the manuscript.

References

- [1] M. Lang, M. Beg, O. Hovorka, and H. Fangohr, arXiv:2203.13689.
- [2] K. Everschor-Sitte, J. Masell, R. M. Reeve, and M. Kläui, *Journal of Applied Physics* **124**, 240901 (2018).
- [3] N. Kent, N. Reynolds, D. Raftrey, I. T. G. Campbell, S. Virasawmy, S. Dhuey, R. V. Chopdekar, A. Hierro-Rodriguez, A. Sorrentino, E. Pereiro, S. Ferrer, F. Hellman, P. Sutcliffe, and P. Fischer, *Nat Commun* **12**, 1562 (2021).
- [4] M. Riou, J. Torrejon, B. Garitane, F. Abreu Araujo, P. Bortolotti, V. Cros, S. Tsunegi, K. Yakushiji, A. Fukushima, H. Kubota, S. Yuasa, D. Querlioz, M. D. Stiles, and J. Grollier, *Phys. Rev. Applied* **12**, 024049 (2019).
- [5] J. Zázvorka, F. Jakobs, D. Heinze, N. Keil, S. Kromin, S. Jaiswal, K. Litzius, G. Jakob, P. Virnau, D. Pinna, K. Everschor-Sitte, L. Rózsa, A. Donges, U. Nowak, and M. Kläui, *Nat. Nanotechnol.* **14**, 658 (2019).
- [6] D. Pinna, G. Bourianoff, and K. Everschor-Sitte, *Phys. Rev. Applied* **14**, 054020 (2020).
- [7] I. Dzyaloshinsky, *Journal of Physics and Chemistry of Solids* **4**, 241 (1958).
- [8] M. Beg, R. A. Pepper, D. Cortés-Ortuño, B. Atie, M.-A. Bisotti, G. Downing, T. Kluyver, O. Hovorka, and H. Fangohr, *Sci Rep* **9**, 7959 (2019).
- [9] R. G. Elías and A. Verga, *Eur. Phys. J. B* **82**, 159 (2011).
- [10] O. V. Pylypovskiy, D. D. Sheka, and Y. Gaididei, *Phys. Rev. B* **85**, 224401 (2012).
- [11] T. B. Winkler, K. Litzius, A. de Lucia, M. Weißenhofer, H. Fangohr, and M. Kläui, *Phys. Rev. Applied* **16**, 044014 (2021).
- [12] A. De Lucia, K. Litzius, B. Krüger, O. A. Tretiakov, and M. Kläui, *Phys. Rev. B* **96**, 020405 (2017).
- [13] C. Andreas, A. Kákay, and R. Hertel, *Phys. Rev. B* **89**, 134403 (2014).
- [14] A. De Lucia, B. Krüger, O. A. Tretiakov, and M. Kläui, *Phys. Rev. B* **94**, 184415 (2016).
- [15] A. Thiaville, J. M. García, R. Dittrich, J. Miltat, and T. Schrefl, *Phys. Rev. B* **67**, 094410 (2003).
- [16] F. N. Rybakov, A. B. Borisov, S. Blügel, and N. S. Kiselev, *Phys. Rev. Lett.* **115**, 117201 (2015).
- [17] F. Tejo, R. H. Heredero, O. Chubykalo-Fesenko, and K. Y. Guslienko, *Sci Rep* **11**, 21714 (2021).
- [18] A. S. Savchenko, F. Zheng, N. S. Kiselev, L. Yang, F. N. Rybakov, S. Blügel, and R. E. Dunin-Borkowski, *APL Materials* **10**, 061110 (2022).
- [19] A. A. Thiele, *Phys. Rev. Lett.* **30**, 230 (1973).
- [20] G. Selke, *Design and Development of a GPU-Accelerated Micromagnetic Simulator* (2014).
- [21] B. Kruger, G. Selke, A. Drews, and D. Pfannkuche, *IEEE Trans. Magn.* **49**, 4749 (2013).
- [22] M. Frigo and S. G. Johnson, in *Proceedings of the 1998 IEEE International Conference on Acoustics, Speech and Signal Processing, ICASSP '98 (Cat. No.98CH36181)*, Vol. 3 (IEEE, Seattle, WA, USA, 1998), pp. 1381–1384.
- [23] S. Woo, K. Litzius, B. Krüger, M.-Y. Im, L. Caretta, K. Richter, M. Mann, A. Krone, R. M. Reeve, M. Weigand, P. Agrawal, I. Lemesh, M.-A. Mawass, P. Fischer, M. Kläui, and G. S. D. Beach, *Nature Mater* **15**, 501 (2016).
- [24] L. Landau and E. Lifshitz, in *Perspectives in Theoretical Physics* (Elsevier, 1992), pp. 51–65.
- [25] T. L. Gilbert, *IEEE Trans. Magn.* **40**, 3443 (2004).
- [26] D. Suess, C. Vogler, F. Bruckner, P. Heistracher, F. Slanovc, and C. Abert, *Sci Rep* **9**, 4827 (2019).
- [27] M. Charilaou, *Phys. Rev. B* **102**, 014430 (2020).
- [28] Y. Li, L. Pierobon, M. Charilaou, H.-B. Braun, N. R. Walet, J. F. Löffler, J. J. Miles, and C. Moutafis, *Phys. Rev. Research* **2**, 033006 (2020).

- [29] W. Döring, Journal of Applied Physics **39**, 1006 (1968).
- [30] B. Berg and M. Lüscher, Nuclear Physics B **190**, 412 (1981).
- [31] K. Yu. Guslienko, B. A. Ivanov, V. Novosad, Y. Otani, H. Shima, and K. Fukamichi, J. Appl. Phys. **91**, 8037 (2002).
- [32] R. Antos and Y. Otani, *The Dynamics of Magnetic Vortices and Skyrmions*, Vol. 1 (Oxford University Press, 2017).